Communication in Physical Sciences 2020, 5(3): 246-256 https://journalcps.com

Investigation of the Inhibition of the Corrosion of carbon steel in Solution of HCl by Glimepiride

*Nkem B. Iroha and Richard A. Ukpe

Received 26 April 2020/Accepted 21 May 2020/Published online: 30 May 2020

Abstract *The corrosion inhibition effect of glimepiride (GMP) on the corrosion of X70 carbon steel in 1 M HCl solution was investigated using weight loss, potentiodynamic polarization (PDP), electrochemical impedance spectroscopy (EIS) and scanning electron microscope (SEM) techniques. The inhibition efficiency was found to increase with increase in inhibitor concentration but decreased with temperature rise. The inhibition efficiency of glimepiride ranged from 54.2 to 95.8% for weight loss measurement, 52.0 to 90.5% for PDP and 53.3 to 90.3% for EIS method at 303 K. Polarization studies give evidence that GMP behaves as a mixed type inhibitor but predominantly anodic. Electrochemical impedance spectroscopy (EIS) spectra exhibit one capacitive loop indicating that, the corrosion reaction is controlled by charge transfer process. It was found that the investigated drug acts via adsorption on the carbon steel surface and obeys Langmuir and Temkin adsorption isotherms. Surface studies ascertain that a protective film was formed on the X70 carbon steel surface. The results have clearly shown that glimepiride has the inhibiting capacity for reducing the corrosion of X70 carbon steel in HCl solution.*

Keywords: *Corrosion, inhibition, carbon steel, glimepiride, gravimetric, potentiometric, EIS and SEM techniques.*

*Nkem B. Iroha
Electrochemistry and Material Science Unit
Department of Chemistry
Bayelsa State, Nigeria
Email: irohanb@fuotuoke.edu.ng
Orcid id: 0000-0002-9111-5932

Richard A. Ukpe
Department of Chemistry
Federal University, Otuoke, P. M. B. 126,
Yenagoa, Bayelsa State, Nigeria
Email: ukpera@fuotuoke.edu.ng
Orcid id: 0000-0002-1010-4933

1.0 Introduction

The high strength and cost effectiveness of carbon steel makes it useful as a material of choice for the construction of industrial pipelines and oil-well processing equipment in the oil and gas industry (Onyeachu *et al*., 2019). Acid solutions are often used in some industrial processes such as oil-well acidizing, acid cleaning and acid pickling (Zaafarany and Ghulman, 2013). Consequently, the metal is exposed to corrosion attack. Metals corrode when they come in contact with aggressive medium such as acid, alkaline and salt solutions (Verma *et al*., 2016). Inhibition of the corrosion of carbon steel is necessary because of the economic cost of replacing corroded facilities made from carbon steel. Although there are several options that have been adopted for controlling the corrosion of carbon steel in acidic medium, the use of corrosion inhibitors is one of the best options (Jisha *et al.,* 2019). A corrosion inhibitor is any compound that retards the rate of corrosion of a metal when added in a minute concentration (Iroha and Hamilton-Amachree, 2019). Studies have shown that the initial mechanism for any corrosion inhibition process is the adsorption of the inhibitor on the metal surface (Singh and Quraishi, 2010). The adsorption may involve the transfer of charge from charged inhibitor to charged metal surface (physiosorption) or the transfer of electron from the inhibitor to the metal surface (Daoud et al., 2015; Abdallah, 2004). Most corrosion inhibitors are organic compounds that possess one or more of the following properties, atoms, π-electron, multiple bonds, conjugated system, aromatic system, suitable functional groups and high molecular mass (Goulart *et al*., 2013). Based in this criterion, several organic compounds have been chosen or synthesized and applied as corrosion inhibitors for metals including carbon steel (Lagrene *et al*., 2002; Musa *et al.*, 2011; Iroha *et al*., 2005). However, one of the greatest challenges in the corrosion industries is the need to discover corrosion

inhibitors whose optimum performance is matched with environmental and other requirements such as cost, ease of availability, biodegradability, non-toxicity and eco-friendliness (Hussin and Kassim, 2011). According to Ebenso and Eddy (2008), green corrosion inhibitors meet these requirements and that investigation into their inhibition abilities and subsequent industrial applications is highly recommended. Extract of living things have been found to be one of the most demanding green corrosion inhibitors (Ahamed *et al*., 2019; Iroha and James, 2018). Others such as natural polymers have also been reported as good corrosion inhibitor. According to Eddy and Ebenso (2010), the major challenges involved in the use of plant extract as corrosion inhibitor is the elucidation of the actual chemical components that causes the inhibition and since the inhibition properties also depends on several electronic and molecular variables, they advocated the use of drugs. Most drugs have been found to be good corrosion inhibitors including tarivid (Eddy and Ebenso, 2010), cefepime (Iroha and Nnanna, 2019), mebendazole (Ahamad and Quraishi, 2010), etc

Glimepiride (GMP) belongs to a group of drugs called sulfonylurea and is used in the treatment of diabetes mellitus. Its mode of action is by increasing the amount of insulin released from the pancreas (Davis, 2004). GMP has been found to exhibit very low toxicity to the human system. Therefore, the present study is aimed at using glimepiride drug for the inhibition of the corrosion of carbon steel in solution of HCl. The molecular structure of the drug is shown in Fig. 1.

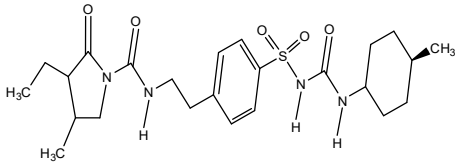

Fig. 1: Chemical structures of glimepiride (3-ethyl-4-methyl-N-(4-(N-(4-methylcyclohexyl carbamoyl)sulfamoyl)phenethyl)-2-oxopyrrolidine-1-carboxamide)

The presence of aromatic ring, hetero atoms (N, S, O) and pi-electrons favour the interaction of the drug with the metal. Weight loss, potentiodynamic polarization (PDP), electrochemical impedance spectroscopy (EIS) and scanning electron microscopy shall be used to investigate the corrosion inhibition properties of glimepiride.

2.0 Materials and Methods

2.1. Materials

The sheet of X70 steel used for this study has the following chemical composition (wt. %): C, 0.26; Mn, 1.65; P, 0.030; S, 0.030; Fe, 98.03 and was obtained from Shell Nigeria oil field. The test specimens were cut into dimension 2 x 4 x 0.2 cm for weight loss measurement and 1 x 2 x 0.2 cm for electrochemical measurements. For the weight loss measurements, a 2 mm diameter small hole was drilled near the upper edge of the specimen to accommodate a suspension hook. Prior to the measurements the test specimens were polished with various grades of emery papers (600 - 1200 grades) and then washed with distilled water and acetone as recommended by ASTM standard G -1-72. The blank corrodent was 1 M HCl solution prepared by dilution of analytical grade HCl (37%) with double distilled water. The glimepiride drug was prepared in the concentrations of 0.1, 0.2, 0.3, 0.4 and 0.5 mM.

2.2. Weight Loss Analysis

The pre-cleaned and weighed coupons were suspended in 250 mL beaker, which contained 100 mL of the test using glass hooks and rods at 303 K. After 4 hours of immersion, the samples were withdrawn and washed with distilled water and ethanol, and then dried and weighed. The experiments were repeated at 313 and 323 K. From the weight loss, the corrosion rate (C_R) (mg cm^{-2} h^{-1}) was calculated using equation 1 (Chaieb, *et al.,* 2009):

$$C_R = \frac{\Delta W}{At} \qquad (1)$$

where ΔW is the weight lost ($\Delta W = w_i - w_f$), w_i and w_f represent the initial and final (after 4 h immersion time) weight of the X70 steel specimens, respectively, A is the surface area of the coupon (cm^2) and t is the period of exposure (h). The inhibition efficiency ($\eta_{WL}\%$) and surface coverage (θ) values were calculated using equations 2 and 3 respectively.

$$\eta_{WL}\% = \frac{C_R^o - C_R^i}{C_R^o} \times 100 \qquad (2)$$

$$\theta = \frac{C_R^o - C_R^i}{C_R^o} \qquad (3)$$

where C_R^o and C_R^i are the values of the corrosion rates

of X70 steel in the absence and presence of inhibitor, respectively.

2.3 *Electrochemical methods*

For electrochemical studies, Autolab galvanostat/ potentiostat (PGSTAT) model 302 N obtained from Metrohm was used. Different tests were conducted to investigate the corrosion behavior of the X70 steel in the presence and absence of the inhibitor. In all electrochemical tests, a three-electrode cell assembly, consisting of X70 steel as a working electrode with 1.0 cm^2 exposed area, platinum as a counter electrode and saturated calomel electrode (SCE) as a reference electrode were employed. The electrochemical system was maintained in an unperturbed state for a period of 30 minutes in order to allow it to attend the steady open circuit potential (OCP) before each electrochemical measurement. Each experiment was carried out in triplicate and the average values of corrosion parameters are reported. Tafel curves were obtained by changing the electrode potential automatically from −250 to +250 mV versus OCP at a scan rate of 10 mV s^{-1}. EIS measurements were carried out in a frequency range from 100 kHz to 10 mHz under potentiodynamic conditions, with amplitude of 10 mV peak-to-peak, using AC signal at E_{corr}. Simulation of results and fitting of the curve are done using the built-in software of the electrochemical work station.

2.4 *Surface morphological Studies*

The surface morphology of the X70 steel immersed in 1 M HCl solution with or without a 0.5 mM GMP inhibitor was observed by using scanning electron microscope (SEM) Supra 40, Carl Zeiss, Germany. After 4 h of immersion in the test solutions, the steel specimens were taken out, washed with double distilled water, dried and finally analysed by SEM method.

3.0 Results and Discussion

3.1 *Weight Loss Study*

3.1.1 Effect of inhibitor concentration

Fig. 2 shows the variation of corrosion rate with concentration for the corrosion of carbon steel in the absence and presence of various concentrations of GMP at 303, 313 and 323 K for X70 steel upon immersion in 1 M HCl in the presence and absence of different concentrations of the inhibitor at 303, 313 and 323 K. The plots reveal that the higher the concentration of GMP, the lower the corrosion rate. However, the higher the temperature the higher the corrosion rate. The percentage inhibition efficiency ($\eta_{WL}\%$) at 303, 313 and 323 K are presented in Tables 1. The $\eta_{WL}\%$ increases with increase in the concentration of the inhibitor but decreased with increasing temperature indicating that GMP is an adsorption inhibitor for the corrosion of carbon steel in solution of HCl. Adsorption inhibitor is characterized by increase in of inhibition efficiency with concentration. The mechanism of adsorption of the inhibitor is physical adsorption because the extent of adsorption decreases with increase in temperature (Muthukrishnan *et al*., 2015; Tao *et al*., 2012; Hamilton-Amachree and Iroha, 2019).

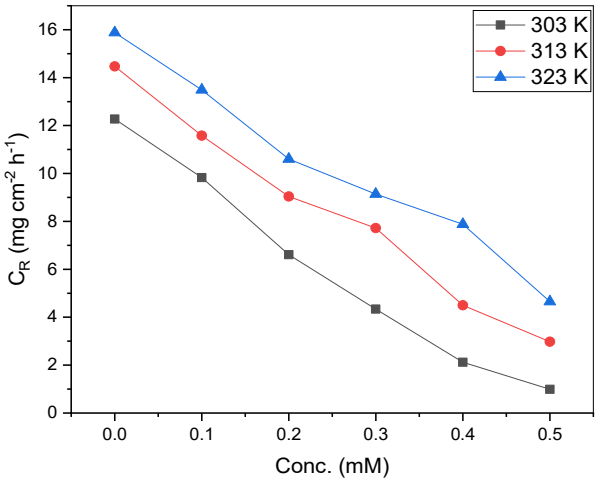

Fig. 2: Variation of corrosion rate with concentration for the corrosion of carbon steel in 1 M HCl containing various concentrations of GMP at various temperatures.

Table 1: Inhibitor efficiency ($\eta_{WL}\%$) of GMP for carbon steel in 1 M HCl at various temperatures.

Inhibitor Conc. (mM)	303 K $\eta_{WL}\%$	313 K $\eta_{WL}\%$	323 K $\eta_{WL}\%$
0.1	54.2	50.8	47.6
0.2	62.7	59.2	55.3
0.3	74.4	71.7	68.9
0.4	88.6	83.3	72.6
0.5	95.8	91.9	87.9

3.1.2 Effect of temperature

The effect of temperature on the rate of corrosion of X70 steel in 1 M HCl containing different concentrations of GMP was tested by weight loss measurements over a temperature range from 303 to 323 K. Plot of inhibition efficiency versus

temperature depicted in Fig. 3, showed that the inhibition efficiency was decreased with a rise in temperature, which suggest that the inhibitor is physically adsorbed on the metal surface. The relation between the corrosion rate (C_R) of X70 steel in acidic media and temperature (T) is often expressed by the Arrhenius equation as follows (Madueke and Iroha, 2018):

$$C_R = A\ exp\left(\frac{-E_a}{RT}\right) \qquad (4a)$$

where E_a is the apparent activation corrosion energy, R is the universal gas constant, A is the pre-exponential factor and T is the absolute temperature. The logarithm for of the Arrhenius equation can be expressed according to equation 4b as follows:

$$logC_R = logA - \frac{E_a}{2.303RT} \qquad (4b)$$

Therefore, the fitness of Arrhenius model to the corrosion data requires that a plot of log (C_R) versus 1/T should be linear. Fig. 4 shows the Arrhenius plots for the corrosion of X70 steel in 1 M HCl in the presence and absence of GMP. Activation energies for various concentrations of GMP are recorded in Table 2. The results indicated that the activation energy increases with concentration indicating that there is increasing ease of adsorption with increasing concentration. Also, the activation energy for the blank was lower than those obtained in the presence of GMP indicating that the corrosion of carbon steel is retarded by GMP. Thermodynamic parameters for the adsorption of GMP on the surface of the metal were calculated using the Transition state equation (equation 5) (Eddy and Ita, 2011).

$$C_R = \frac{RT}{Nh}\ exp\left(\frac{\Delta S^*}{R}\right)\ exp\left(\frac{-\Delta H^*}{RT}\right) \qquad (5)$$

where ΔS^* is the entropy of activation, ΔH^* is the enthalpy of activation, N is Avogadro's number, and h is Planck's constant. The values of ΔH^* were deduced from the slope, -ΔH/2.303R of the plot of log CR/T against 1/T (Fig. 5) while ΔS^* was evaluated from the intercept, [log (R/Nh) + (ΔS^*/2.303R)] of the same plot. These values are also presented in Table 2. Positive value of activated enthalpy, ΔH^* means that the process is an endothermic process and it needs more energy to achieve the activated state or equilibrium state (Hussin and Kassim, 2011; James and Iroha, 2019). The values of change in activation entropy, ΔS^*, in the presence of the inhibitor are large and negative indicating that the adsorption of the inhibitor occurs with increasing degree of orderliness (Yadav *et al*., 2013).

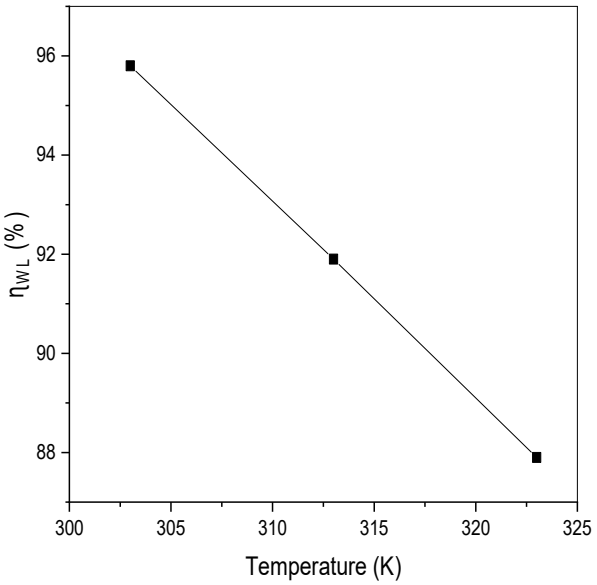

Fig. 3: Variation of inhibition efficiency (η_{WL}%) with temperature for X70 Steel corrosion in 1 M HCl at the optimum concentration of GMP (0.5 mM).

Table 2: Activation parameters for X70 steel corrosion in 1 M HCl without and with different concentrations of GETM

Conc. (mM)	E_a $(kJ\ mol^{-1})$	ΔH^* $(kJ\ mol^{-1})$	ΔS^* $(J\ mol^{-1}\ K^{-1})$
Blank	27.82	22.42	-226.91
0.1	31.75	25.81	-221.92
0.2	33.01	27.93	-220.25
0.3	35.42	28.66	-217.26
0.4	36.59	30.17	-215.39
0.5	38.36	31.84	-213.01

3.1.3: Adsorption Studies

The primary step in the action of inhibitors in alkaline solution is generally agreed to be

adsorption on the metal surface. Adsorption isotherms are employed to understand the adsorption behaviour of the inhibitor. The surface coverage values obtained were applied to various adsorption isotherm models and correlation coefficient (R^2) was used to determine the best fitted adsorption isotherm. The test indicated that the adsorption of GMP on carbon steel surface best fitted the Langmuir adsorption isotherm, which can be expressed as (Iroha and Chidiebere, 2017; Ameer and Fekry, 2010):

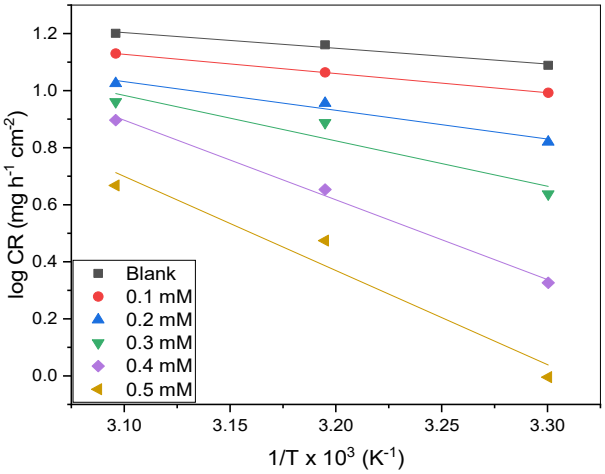

Fig. 4: Arrhenius plots for the corrosion of carbon steel in 1 M HCl containing various concentrations of GMP.

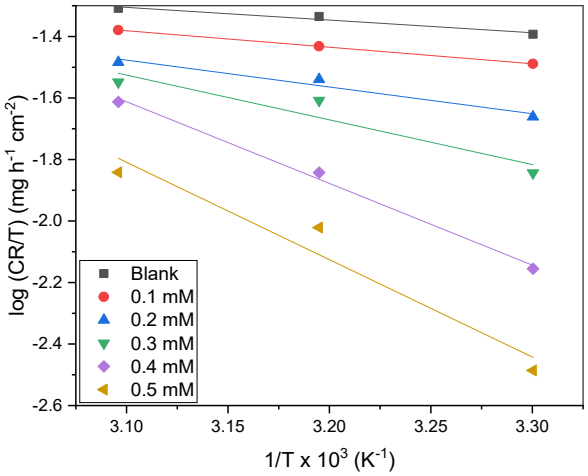

Fig. 5: Transition state plots for the corrosion of carbon steel in 1 M HCl containing various concentrations of GMP.

$$\frac{C_i}{\theta} = \frac{1}{K_{ads}} + C_i \qquad (6)$$

where θ is the degree of the surface coverage, C_i is the concentration of inhibitor in the bulk solution, and K_{ads} is the equilibrium constant of the process of adsorption. A plot of C_i/θ versus C_i (Fig. 6) yielded straight lines with intercepts, $1/K_{ads}$. Slope values ranged from 0.8073 to 0.9068 between 303 to 323 K respectively. This indicates that the adsorption shifted more towards the Langmuir type as the temperature increase. The ideal Langmuir isotherm requires that the slope should be equal to unity, which transforms to the absence of interaction between the adsorbed species. Slope values greater or less than unity indicate that there is interaction between the adsorbed species (Eddy *et al*., 2011a).

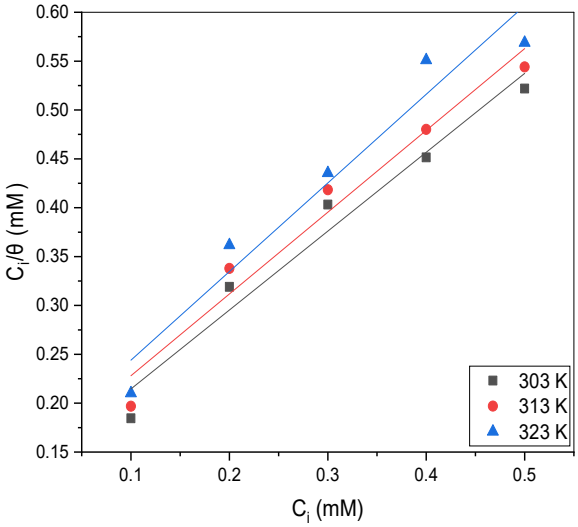

Fig. 6: Langmuir isotherm for the adsorption of GMP on carbon steel surface

Table 3: Langmuir parameters for the adsorption of GMP unto the surface of carbon steel

T (K)	Slope	R^2	K_{ads}	ΔG^o_{ads} (k
303	0.8073	0.9634	0.1338	-5.05
313	0.8368	0.9651	0.1444	-5.42
323	0.9068	0.9466	0.1534	-5.40

Therefore, other adsorption isotherms that consider lateral interaction were considered. The Temkin model can be expressed as follows (Eddy *et al*., 2014; Ukpe, 2019):

$$\exp(-2a\theta) = b_{ads}C \qquad (7)$$

The logarithm of both sides of equation 7 gives a linear model of the Temkin equation (equation 7)

$$\theta = \frac{-2.303}{2a} log b_{ads} - \frac{2.303}{2a} logC \qquad (8)$$

Equation 8 indicates that a plot of θ versus log C should be linear with slope and intercept equal to $\frac{2.303}{2a}$ and $\frac{2.303}{2a}$ respectively. The Temkin isotherm for the adsorption of GMP on the surface of the carbon steel is shown in Fig. 7 while Table 4 presents Temkin adsorption parameters. The observed high degree of linearity (R^2 range from 0.9292 to 0.9373) confirms that the Temkin model is applicable to the adsorption of GMP on carbon steel surface. The interaction parameters were positive indicating the attractive behaviour of the inhibitors (Ukpe, 2019).

The equilibrium constant of adsorption obtained from the Langmuir and Temkin isotherms is related to the standard free energy change of adsorption according to equation 9.

$$K_{ads} = \frac{1}{55.5} exp\left(-\frac{\Delta G^o_{ads}}{RT}\right) \quad (9)$$

where ΔG^o_{ads} is the standard free energy of adsorption, R is the molar gas constant and T is the absolute temperature. Adsorption parameters obtained from this isotherm are listed in Tables 3 and 4.

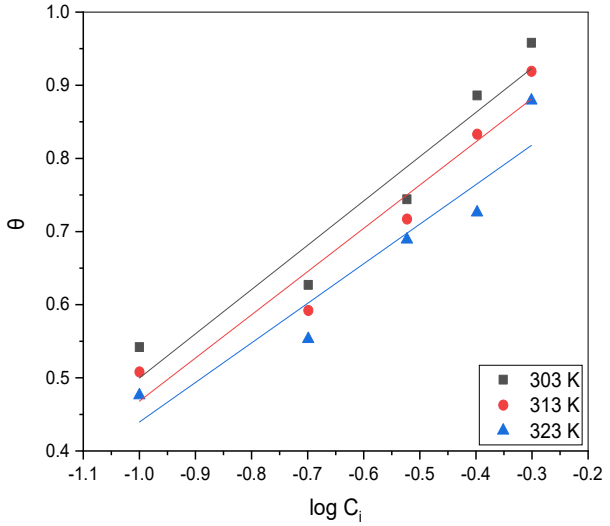

Fig. 7: Temkin isotherm for the adsorption of GMP on the surface of carbon steel

Table 4: Temkin parameters for the adsorption of GMP on the surface of carbon steel

T (K)	a	log K_{ads}	ΔG^o_{ads} (kJ/mol)	R^2
303	0.5257	1.8254	-20.71	0.9292
313	0.5132	1.7922	-21.19	0.9373
323	0.4699	1.8124	-22.00	0.9070

The values of free energy of adsorption (ΔG^o_{ads}) obtained through the Langmuir and Temkin isotherms ranged from -5.05 to -5.42 kJ/mol and from -20.00 to -20.71 kJ/mol respectively. Therefore, the adsorption of GMP on the surface of carbon steel is spontaneous and favours the mechanism of physical adsorption (Eddy *et al*., 2011b).

3.2 Potentiodynamic polarization curves

Anodic and cathodic polarization curves for mild steel corrosion in the absence and presence of GMP at 303 K are shown in Fig. 8. The electrochemical parameters calculated from the related potentiodynamic polarization curves are listed in Table 5. These include, corrosion potential (E_{corr}), corrosion current density (i_{corr}), corrosion inhibition efficiency (η_{PDP}), anodic and cathodic Tafel slope (β_a and β_c). The results indicated a decrease in corrosion current with concentration of GMP indicating that GMP retarded the corrosion of carbon steel in solution of HCl by blocking the active sites on the steel surface through the formation of adsorbed film of the molecules (Cookey *el al*., 2018; Eddy *et al*., 2018). The Tafel constants were also observed to decrease with increase in concentration of GMP indicating that both anodic metal dissolution and cathodic reduction reactions are inhibited by various concentrations of (El-Hajjaji *et al*., 2019). Fig. 8 reveals that the presence of GMP molecules shows much more dominant effect on the anodic reactions as compared to the cathodic reactions. The inhibition efficiency ($\eta_{PDP}\%$) was calculated from polarization measurements using the relation:

$$\eta_{PDP}\% = \left[\frac{i^o_{corr} - i_{corr}}{i^o_{corr}}\right] \times 100 \quad (10)$$

where i^o_{corr} and i_{corr} are the corrosion current densities in the absence and the presence of GMP, respectively. The results in Table 4 show that corrosion current density decreased and the inhibition efficiency ($\eta_{PDP}\%$) increases as the concentration of GMP is increased. This observation can be attributed to the blockage of active sites on the steel surface by the adsorbed film of the molecules of the studied drug (Cookey *el al*., 2018). The maximum shift in E_{corr} for the inhibitor is less than 85 mV, which suggests that the studied drug is mixed-type inhibitor but with anodic predominance (Tayebi *et al*., 2014). At various concentrations of GMP, the values of anodic Tafel slopes are more affected than the slopes value of cathodic Tafel

curves. This finding also suggests that though GMP acts as a mixed type inhibitor, it is predominantly anodic.

3.3: Electrochemical Impedance Spectroscopy (EIS) Studies.

The anticorrosion activity of X70 steel in 1M HCl solution in the absence and presence of various concentrations of GMP was also investigated using EIS measurements at room temperature. The Nyquist impedance spectra of X70 steel immersed in various solutions of HCl are shown in Fig. 9. From the plots, it is evident that the addition of GMP increases the diameter of the arc indicating that there is increasing resistant to corrosion in the presence of various concentration of GMP. The size of the impedance diagram increases as the concentration rises and consequently the inhibition efficiency increases due to the adsorption of inhibitor molecules on the metal surface (Solmaz, 2010; Zarrouk *et al.,* 2015).

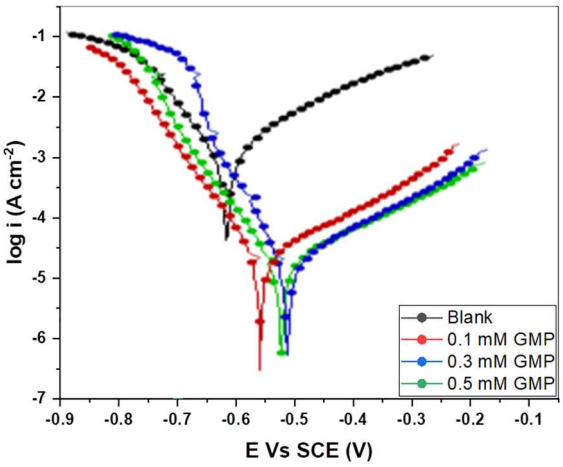

Fig. 8: Polarization curves for X70 steel in 1 M HCl containing various concentrations of GMP.

Table 5: Tafel polarization parameters and $\eta_{PDP}\%$ for the corrosion of X70 steel in 1 M HCl without and with GMP.

Concentration (mM)	$-E_{corr}$ (mV/SCE)	i_{corr} (μA cm^{-2})	β_a (mV dec^{-1})	β_c (mV dec^{-1})	η_{PDP} (%)
0	528	836.4	271.3	122.7	-
0.1	501	401.7	182.9	118.1	52.0
0.3	479	236.3	168.2	121.2	71.7
0.5	465	79.8	161.4	103.5	90.5

The Nyquist plots exhibit depressed capacitive loop, which may be attributed to the charge transfer reaction (Iroha and James, 2019). The depression of the Nyquist semicircles is often associated with the frequency dispersion of interfacial impedance arising from inhomogeneity of the electrode surface due to roughness and/or other interfacial phenomena (Mashuga *et al*., 2015). The Nyquist curves shown in Fig. 9 were fitted by equivalent electrical circuit model as shown in Fig. 10 to survey the mechanism and kinetics of the systems studied. The equivalent circuit contains a solution resistance (R_s) connected to a constant phase element (CPE) which is in parallel with a charge transfer resistance (R_{ct}). The CPE is often used to substitute the double-layer capacitance (C_{dl}) to give a more accurate fit of the experimental impedance data. The CPE-type impedance constituting of component Y_0 and a coefficient n is given as (Bustamante *et al*., 2009)

$$Z_{CPE} = \frac{1}{Y_o}(j\omega)^{-n} \qquad (11)$$

where Y_0 is a proportionality factor, $j = (-1)^{\frac{1}{2}}$ which is an imaginary number, ω is the angular frequency in rad/s, and n has the meaning of a phase shift. For n = 0, CPE represents a resistance, for n =1 a capacitance and for n = –1 an inductance. The double layer capacitance (C_{dl}) and inhibition efficiency ($\eta_{EIS}\%$) are calculated as follows:

$$C_{dl} = Y_o(\omega_{max})^{n-1} \qquad (12)$$

$$\eta_{EIS}\% = \frac{R_{ct}^{i} - R_{ct}^{o}}{R_{ct}^{i}} \times 100 \qquad (13)$$

where ω_{max} is the angular frequency at which the imaginary part of the impedance has a maximum. R_{ct}^{o} and R_{ct}^{i} are the charge-transfer resistances in the absence and presence of the inhibitors, respectively. The calculated impedance impedance parameters are given in Table 5. The results in Table 5 demonstrates that, on increasing GMP concentration, the charge transfer resistance (R_{ct}) increased and double layer capacitance (C_{dl}) decreased leading to an increase in inhibition efficiency. The decrease in C_{dl} results from a

decrease in local dielectric constant and/or an increase in the thickness of the double layer, suggesting that GMP molecules have been adsorbed at the interface (Lagrenee et al. 2002). Increase in R_{ct} shows that a charge transfer process is mainly controlling the corrosion of X70 steel in acidic media. The inhibition efficiency (η_{EIS}%) of the GMP inhibitor determined by three different methods, weight loss, polarization and electrochemical impedance spectroscopy, as a function of concentration are in coherence with each other.

Table 6: Impedance parameters for the corrosion of X70 steel in 1 M HCl in the absence and presence of different concentrations of GMP at 303 K.

Concentration (mM)	R_s (Ω cm^2)	R_{ct} (Ω cm^2)	Y_o ($\mu\Omega^{-1}$ s^n cm^{-2})	C_{dl} (μF cm^{-2})	n	η_{EIS} (%)
0	1.29	32.6	301.6	221.8	0.905	
0.1	1.17	69.8	269.3	172.9	0.914	53.3
0.3	1.01	112.3	243.1	148.3	0.920	71.0
0.5	0.87	337.5	235.0	113.4	0.9929	90.3

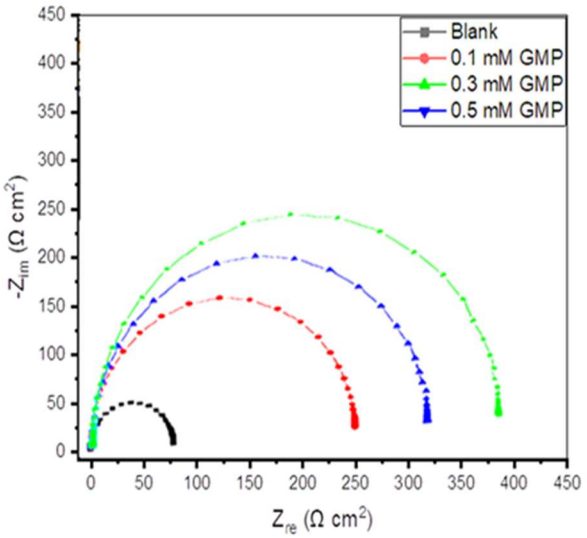

Fig. 9: Nyquist plot for X70 steel corrosion in different concentrations of GMP at 303 K.

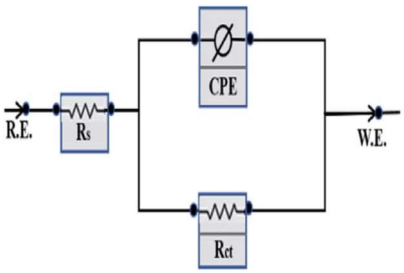

Fig. 10: Equivalent circuit used to fit the EIS experiment data.

3.4: Scanning Electron Microscope (SEM) Studies

The scanning electron micrographs of carbon steel before and after corrosion inhibition are shown in Fig. 11a and 11b respectively. (Fig. 11a) shows a damaged rough surface with cracks and pits due to the attack of corrosive solution. Fig.10b shows the micrograph of X70 carbon steel specimen immersed in 1 M HCl containing 0.5mM GMP, which reveals a remarkably improved surface with comparatively smooth and less corroded surface which might be attributed to the formation of protective film by GMP molecules on metal surface.

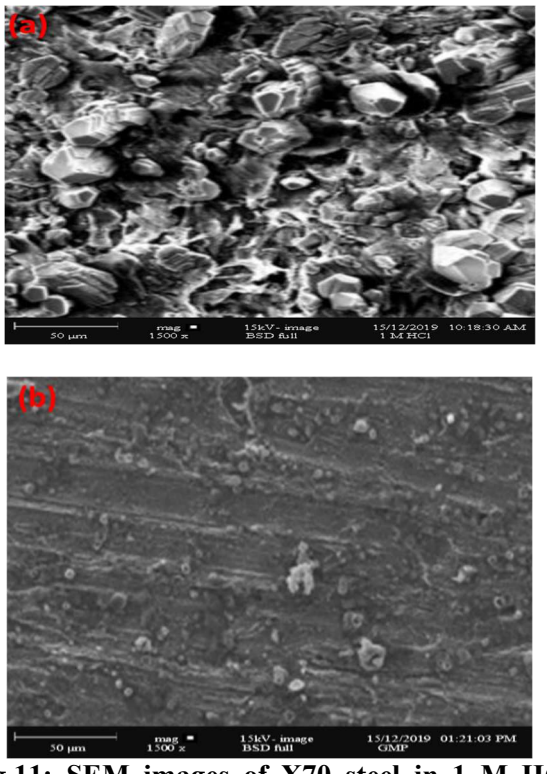

Fig.11: SEM images of X70 steel in 1 M HCl solution after 4 h immersion time: (a) in absence of GMP and (b) in the presence of 0.5 mM GMP.

The micrograph of the carbon steel without inhibitor

4.0 Conclusion

Glimepiride was examined as corrosion inhibitor for X70 steel in 1 M HCl solution and was found to inhibit the corrosion process by adsorption on the metal/solution interface. The inhibition efficiency of the inhibitor increases with increase in the inhibitor concentration but decreases with rise in temperature. The adsorption of the investigated drug on X70 steel surface in 1 M HCl solution is spontaneous and follows Langmuir adsorption isotherm. Polarization study revealed that GMP was predominantly anodic type inhibitor. EIS studies indicated that R_{ct} values increase while C_{dl} values decrease in presence of GMP. SEM studies confirmed that GMP form protective surface film on the steel surface.

5.0 Reference

Abdallah, M. (2004). Antibacterial Drugs as Corrosion Inhibitors for Corrosion of Aluminium in Hydrochloric Solution. *Corros. Sci.,* 46, pp. 1981–1996.

Ahamed, K. R., Farzana, B. A., Diraviam, S. J., Dorothy, Rajendran, R. S. & Al-Hashem, A. (2019). Mild Steel Corrosion Inhibition by the Aqueous Extract of *Commelina benghalensis* Leaves. *Port. Electrochim. Acta*, 37, pp. 51-70

Ahamad, I. and Quraishi, M. A. (2010). Mebendazole: new and efficient corrosion inhibitor for mild steel in acid medium. Corrosion Science, 52, pp. 651-658.

Ameh, P. O.& Eddy, N. O. (2018). Theoretical and experimental investigations of the corrosion Inhibition action of *Piliostigma thonningii* extract on mild steel in acidic medium. Communication in Physical Sciences 3, 2, pp. 27-42.

Ameer, M. A. & Fekry, A. M. (2010). Corrosion inhibition of mild steel in acidic media using newly synthesized heterocyclic organic molecules. *Int. J. Hydrogen Energy*, 35, pp. 11387–11396.

Awe, F. E., Abdulwahab, M. & Otaru, H. A. (2019). Adsorptive studies of the inhibitive properties of ethanolic extracts of *Parinari polyandra* on mild steel in acidic media. Communication in Physical Sciences, 4, 1, pp. 49-57.

Bustamante, R. A., Silve, G. N., Quijano, M. A., Hernandez H. H., Romo, M. R., Cuan, A., Pardave, M. P. (2009) Electrochemical study of 2-mercaptoimidazole as a novel corrosion inhibitor for steels. Electrochim Acta, 54, pp. 5393–5399.

Chaieb, E., Bouyanzer, A., Hammouti, B. & Berrabah, M. (2009). Limonene as green inhibitor for steel corrosion in Hydrochloric Acid. *Acta Phys. Chim. Sin*., 25, pp. 1254.

Cookey, G. A., Tambari, B. L. & Iboroma, D. S. (2018). Evaluation of corrosion inhibition potentials of green tip forest lily (*Clivia nobilis*) leaves extract on mild steel in acid media. *Journal of applied sci. Env.Mgt.*, 22, 1, pp. 90-94.

Daoud, D., Douadi, T., Hamani, H., Chafaa, S. and Al-noaimi, M. (2015). Corrosion inhibition of mild steel by two new s-heterocyclic compounds in 1 M HCl Experimental and computational study. *Corrosion Science*, 94, pp. 21-37.

Davis, S.N. (2004). The role of glimepiride in the effective management of Type 2 diabetes. *J. Diabetes Complicat.*, 18, 6, pp. 367–76.

Eddy, N. O. & Ebenso, E. E. (2010). Corrosion inhibition and adsorption characteristics of tarivid on mild steel in H2SO4. *E Journal of Chemistry*, 7, S1, pp. S442-S448.

Eddy, N. O, Ibok, U. J., Ameh, P. O., Alobi, N. O. & Sambo, M. M. (2014). Adsorption and quantum chemical studies on the inhibition of the corrosion of aluminum in HCl by *Gloriosa superba* (GS) gum *Chemical Engineering Communications*, 201, 10, pp. 1360-1383

Eddy, N. O. and Ita, B. I. (2011). Theoretical and experimental studies on the inhibition potentials of aromatic oxaldehydes for the corrosion of mild steel in 0.1 M HCl. *Journal of Molecular Modeling* 17, pp. 633-647

Eddy, N. O., Ameh, P. O., Gimba, E. E. & Ebenso, E. E. (2011a). GCMS studies on *Anogessus leocarpus* gum and their corrosion inhibition potential for mild steel in 0.1 M HCl. *International Journal of Electrochemical Sciences*, 6, pp. 5815-5829.

Eddy, N. O, Ekwumengbo, PA, Mamza, PAP (2009c) Ethanol extract of *Terminalia catappa* as a green inhibitor for the corrosion of mild steel in H_2SO_4 *Green Chemistry Letters and Review* 2, 4, pp. 223-231

Eddy, N. O., Ita, B. I., Dodo, S. N., Paul E. D. (2011b). Inhibitive and adsorption properties of ethanol extract of *Hibiscus sabdariffa* calyx for

the corrosion of mild steel in 01 M HCl *Green Chemistry Letters and Review*, 5, 1, pp. 43-53.

Eddy, N. O., Ameh, P. O. and Essien, N. B. (2018). Experimental and computational Chemistry studies on the inhibition of aluminum and mild steel in 0.1 M HCl by 3-nitrobenzoic acid. *Journal of Taibah University for Science*, 12 (5): 545-556

El-Hajjaji, F., Merimi, I., El Ouasif, L., El Ghoul, M., Achour, R., Hammouti, B., Belghitia, M. E., Chauhand, D. S. & Quraishi, M. A. (2019). 1-Octyl-2-(octylthio)-1H-benzimidazole as a New and Effective Corrosion Inhibitor for Carbon Steel in 1 M HCl. *Port. Electrochim. Acta,* 37, pp. 131-145

Goulart, C. M., Esteves-Souza, A., Martinez-Huitle, C. A., Rodrigues, C. J. F., Maciel, M. A. M. and Echevarria, A. (2013). Experimental and theoretical evaluation of semicarbazones and thiosemicarbazones as organic corrosion inhibitors. *Corrosion Science*, 67, pp. 281-291.

Hamilton-Amachree A, Iroha N. B. (2019) Corrosion inhibition of API 5L X80 pipeline steel in acidic environment using aqueous extract of *Thevetia peruviana*. Chem Int 6:117-128.

Hussin, M. H. & Kassim, M. J. (2011). The corrosion inhibition and adsorption behavior of *Uncaria gambir* extract on mild steel in 1M HCl. *Materials Chemistry and Physics*, 125, pp. 461–468.

Iroha, N. B. & Hamilton-Amachree, A. (2019) Inhibition and adsorption of oil extract of *Balanites aegyptiaca* seeds on the corrosion of mild steel in hydrochloric acid environment. *World Sci New,* 126, pp. 183-197.

Iroha, N. B. & James, A. O. (2018). Assessment of Performance of Velvet Tamarind-furfural resin as Corrosion Inhibitor for Mild Steel in Acidic Solution, *J. Chem Soc. Nigeria,* 43, 3, pp. 510 – 517.

Iroha, N. B. & James, A. O. (2019). Adsorption behavior of pharmaceutically active dexketoprofen as sustainable corrosion Inhibitor for API X80 carbon steel in acidic medium. *World News Nat Sciences*, 27, pp. 22-37.

Iroha, N. B. & Nnanna, L. A. (2019). Electrochemical and Adsorption Study of the anticorrosion behavior of Cefepime on Pipeline steel surface in acidic Solution. J. Mater. Environ. Sci. 10, 10, pp. 898-908.

Iroha, N. B., Chidiebere, M. A. (2017) Evaluation of the Inhibitive Effect of Annona Muricata .L Leaves Extract on Low-Carbon Steel Corrosion in Acidic Media. *International Journal of Materials and Chemistry*, 7, pp. 47-54.

Iroha, N. B. Oguzie, E. E. Onuoha, G. N. & Onuchukwu, A. I. (2005) Inhibition of Mild Steel Corrosion in Acidic Solution by derivatives of Diphenyl Glyoxal, *16th International Corrosion Congress, Beijing, China*, pp. 126-131.

James, A. O. & Iroha, N. B. (2019). An Investigation on the Inhibitory Action of Modified Almond Extract on the Corrosion of Q235 Mild Steel in Acid Environment. *IOSR Journal of Applied Chemistry*, 12, 2, pp. 1-10

Jisha, M., Hukuman, N. H. Z., Leena, P. & Abdussalam, A. K. (2019). Electrochemical, computational and adsorption studies of leaf and floral extracts of *Pogostemon quadrifolius* (Benth.) as corrosion inhibitor for mild steel in hydrochloric acid. *J. Mater. Environ. Sci*., 10, 9, pp. 840-853.

Lagrene, M., Mernari, B., Bouanis, M., Traisnel M. & Bentiss, F. (2002). Study of the mechanism and inhibiting efficiency of 3,5-bis(4-methylthiophenyl)-4H-1,2,4-triazole on mild steel corrosion in acidic media. *Corros. Sci.,* 44, 3, pp. 573-588

Ma, Y., Han, F., Li, Z. & Xia, C. (2016). Acidic-Functionalized Ionic Liquid as Corrosion Inhibitor for 304 Stainless Steel in Aqueous Sulfuric Acid. *ACS Sustain. Chem. Eng*., 4, 9, pp. 5046-5052.

Madueke, N. A. & Iroha, N. B. (2018). Protecting Aluminium Alloy of type AA8011 from Acid Corrosion Using Extract from Allamanda cathartica Leaves. *International Journal of Innovative Research in Science, Engineering and Technology,* 7, 10, pp. 10251-10258.

Mashuga, M. E., Olasunkanmi, L. O., Adekunle, A. S., Yesudass, S., Kabanda, M. M. & Ebenso, E. E. (2015). Adsorption, thermodynamic and quantum chemical studies of 1-hexyl-3-methylimidazolium based ionic liquids as corrosion inhibitors for mild steel in HCl. *Materials*, 8, 6, pp. 3607–3632.

Muthukrishnan, P., Prakash, P., Ilayaraja, M., Jeyaprabha, B. & Shankar, K (2015). Effect of Acidified *Feronia elephantum* Leaf Extract on the Corrosion Behavior of Mild Steel. *Metallurgical and Materials Transactions B*, 46b, pp. 1448-1460.

Musa, A. Y., Mohamad, A. B., Khadum, A. A. H. & Chee, E. P. (2011). Galvanic corrosion of aluminum alloy (Al2024) and copper in 1.0 M nitric acid. *Int J Electrochem Sci*, 6, pp. 5052-5065.

Onyeachu, I. B., Chauhan, D. S., Ansari, K. R., Obot, I. B., Quraishi M. A. & Alamri, A. H. (2019). Hexamethylene-1,6-bis(N-D-glucopyranosylamine) as a novel corrosion inhibitor for oil and gas industry: electrochemical and computational analysis. *New J. Chem*., 43, pp. 7282-7293.

Singh, A. K. & Quraishi, M. A. (2010). Effect of Cefazolin on the corrosion of mild steel in HCl solution. *Corrosion Science*, 52, pp. 152–160.

Solmaz, R. (2010). Investigation of the inhibition effect of 5-((E)-4-phenylbuta-1,3-dienylideneamino)-1,3,4-thiadiazole-2-thiol Schiff base on mild steel corrosion in hydrochloric acid. *Corros. Sci.,* 52, pp. 3321–3330.

Tao, Z., Zhang, S., Li, W. & Hou, B. (2011). Adsorption and Inhibitory Mechanism of 1H-1,2,4-Triazol-l-yl-methyl-2-(4-chlorophenoxy) Acetate on Corrosion of Mild Steel in Acidic Solution. *Ind. Eng. Chem. Res.,* 50, 10, pp. 6082–6088.

Tayebi, H., Bourazmi, H., Himmi, B., El Assyry, A., Ramli, Y., Zarrouk, A., Geunbour. A., Hammouti, B., Ebenso, E. E. (2014) An electrochemical and theoretical evaluation of new quinoline derivative as a corrosion inhibitor for carbon steel in HCl solutions. *Der Pharm Lett,* 6, pp. 20–34.

Ukpe, R. A. (2019). Joint effect of ethanol extract of orange peel and halides on the Inhibition of the corrosion of aluminum in 0.1 M HCl: An approach to resource recovery. *Communication in Physical Sciences*, 4, 2, pp. 118-132

Verma, C., Quraishi, M. A., Ebenso, E. E., Obot, I. B. & El Assyry, A. (2016). 3-Amino alkylated indoles as corrosion inhibitors for mild steel in 1M HCl: Experimental and theoretical studies. *Journal of Molecular Liquids*. 219, pp. 647–660.

Yadav, M., Kumar, S., Sinha, R. R. & Behera, D. (2013). Experimental and Quantum Chemical Studies on Corrosion Inhibition Performance of Benzimidazole Derivatives for Mild Steel in HCl. *Ind. Eng. Chem. Res*., 52, pp. 6318

Zaafarany, I. A. & Ghulman, H. A. (2013). Ethoxylated fatty amines as corrosion inhibitors for carbon steel in hydrochloric acid solutions. *Int. J. Corros. Scale Inhib*., 2,2, pp. 82–91.

Zarrouk, A., Hammouti, B., Lakhlifi, T., Traisnel, M., Vezin, H. & Bentiss, F. (2015). New 1H-pyrrole-2,5-dione derivatives as efficient organic inhibitors of carbon steel corrosion in hydrochloric acid medium: Electrochemical, XPS and DFT studies. *Corrosion Science*, 90, pp. 572–584.